THE UNIVERSITY *of* EDINBURGH

Edinburgh Research Explorer

Monitoring intracellular redox potential changes using SERS nanosensors

OPEN ACCESS

Monitoring Intracellular Redox Potential Changes Using SERS Nanosensors**

Craig A. R. Auchinvole,[1] Patricia Richardson,[1] Catherine McGuinnes,[2] Venkatesh Mallikarjun,[1,3] Ken Donaldson,[2] Hamish McNab[1] and Colin J. Campbell.[1,3,]*

[1]EaStCHEM, School of Chemistry, Joseph Black Building, University of Edinburgh, West Mains Road, Edinburgh, EH9 3JJ, UK.

[2]Centre for Inflammation Research, University of Edinburgh, Edinburgh EH16 4TJ.

[3]Division of Pathway Medicine, University of Edinburgh, Edinburgh EH16 5SB.

[*]Corresponding author; C.J.C. e-mail: colin.campbell@ed.ac.uk, tel: 0044 (0)131 242 6471, fax: 0044 (0)131 242 6244

Supporting information:
Synthetic schemes and characterisation data (including electrochemical and computational studies) for HQ and NQ. SERS using redox couples and nanosensor TEM gallery. This material is available free of charge via the Internet at http://pubs.acs.org

Abbreviations:
ROS, reactive oxygen species; roGFP, redox-active green fluorescent protein; NHE, normal hydrogen electrode; SERS, surface enhanced Raman scattering; NS, gold nanoshells; IR, infra-red; NQ, 1,8-diaza-4,5-dithia-1,8-di(2-chloro-[1,4]-naphthoquinone-3-yl)octane; HQ, 2-Mercapto-benzene-1,4-diol; DFT, Density Functional Theory; GSH/GSSG, oxi-dized/reduced glutathione; Cys/CySSyC, oxidized/reduced cysteine; NADP+/NADPH, oxidized/reduced nicotinamide adenine dinucleotide phosphate; TEM, transmission electron microscopy; DMEM, Dulbecco's Modified Eagle Medium; DCFH-DA, dichlorofluorescein-diacetate; t-BuOOH, tertiary-butyl hydroperoxide; AAPH, 2,2'-azobis-2-methyl-propanimidamide, dihydrochloride; SOD, superoxide dismutase; DTT, dithiothreitol; DNA, deoxyribonucleic acid; ER, endoplasmic reticulum; UPR, unfolded protein response; CS, calf serum; TCEP, tris(2-carboxyethyl)phosphine.

Graphical abstract
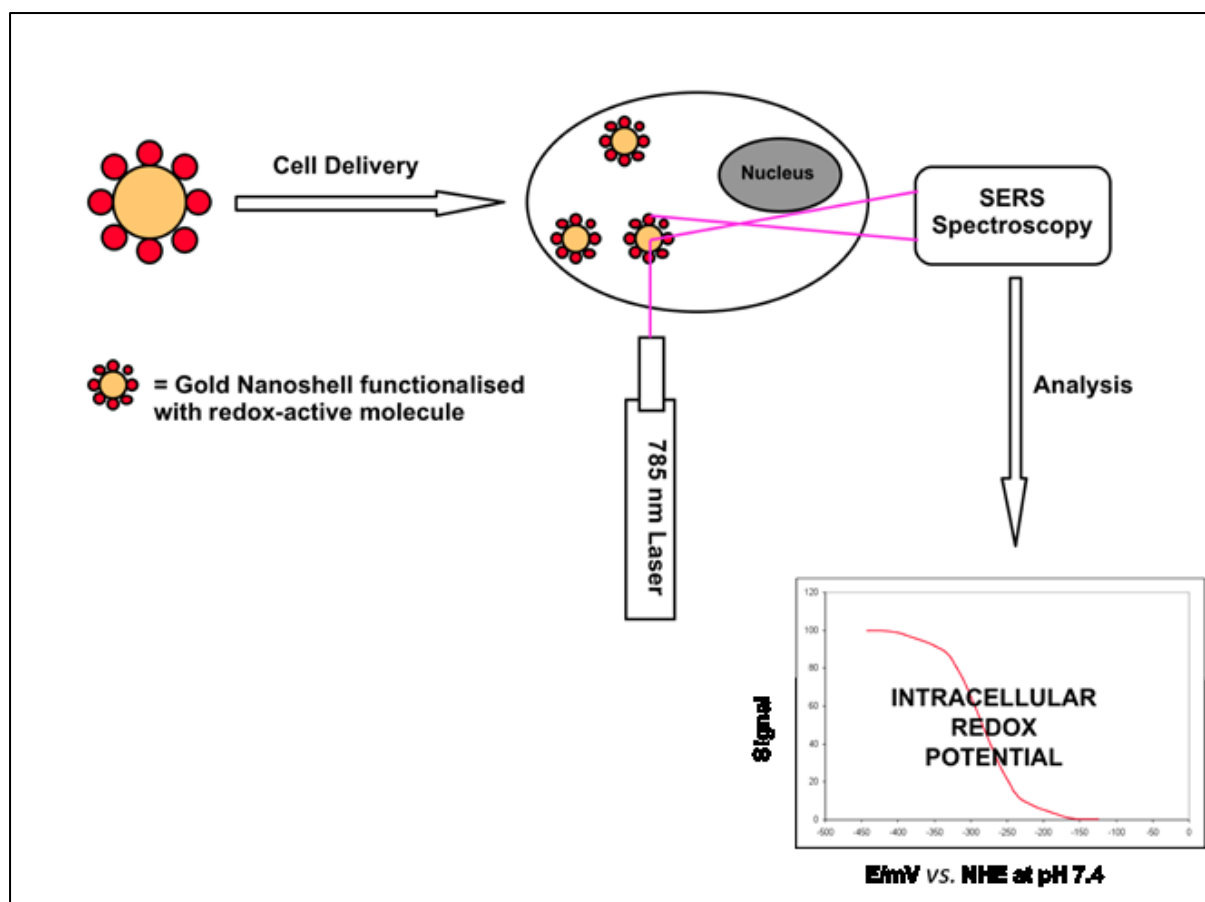
Abstract

Redox homeostasis and signalling are critically important in the regulation of cell function. There are significant challenges in quantitatively measuring intracellular redox potentials and in this paper we introduce a new approach. Our approach is based on the use of nanosensors which comprise molecules which sense the local redox potential, assembled on a gold nanoshell. Since the Raman spectrum of the sensor molecule changes depending on its oxidation state and since the nanoshell allows a huge enhancement of the Raman spectrum, intracellular potential can be calculated by a simple optical measurement. The nanosensors can be controllably delivered to the cytoplasm, without any toxic effects allowing redox potential to be monitored in a reversible, non-invasive manner over a previously unattainable potential range encompassing both superphysiological and physiological oxidative stress.

Introduction

Intracellular redox potential is a highly regulated state which is critically important in cell-cycle, differentiation, apoptosis, inflammation, toxicity, protein-interactions and signalling.[1-5] The disregulation of cellular redox potential, particularly to pro-oxidative states is implicated in the initiation and progression of several disease states including cardiovascular disease, neurodegenerative disease and cancer.[6,7] Despite the importance of intracellular redox potential, its study is severely limited by the lack of suitable measurement techniques.

Intracellular redox potential is a balanced state dependent on a variety of factors including, on one hand, intrinsic and extrinsic reactive oxygen species (ROS) and on the other hand a range of antioxidant mechanisms such as glutathione, thioredoxin, NADPH and cellular pH.[8] The normal function of the cell requires that the redox potentials in cellular organelles are not in equilibrium with one another and while the hypothetical electrochemical window of the cell (determined by NADPH and oxygen) spans more than a volt, subtle changes in potential of as little as 60 mV in a particular organelle may significantly activate a protein or pathway. As a result, in order to gain a full understanding of redox potential in the cell so that it might be modulated for therapeutic gain, there is a need to measure intracellular redox potential quantitatively and with sub-cellular resolution.[7,9]

While optical techniques exist which can give information on localised redox potential they suffer from several drawbacks. Engineered fluorescent protein reporters can be used to monitor localised redox potential,[10] but they are limited to measurements in a narrow potential window (roGFPs have standard reduction potentials between -290 and -230 mV *vs*. NHE)[11] and they have been demonstrated to be insufficiently stable to oxidation to measure the potential of endoplasmic reticulum or endosomal compartments and are thus unlikely to be useful for studies of oxidative stress.[9,11] Protein engineering offers limited opportunities for extension to wider potential ranges compared to small molecule strategies and hence there is a need for complementary approaches.

Although fluorescent dyes (*e.g.* dichlorofluorescein-diacetate[12], and hydrocyanines[13]) have been developed which report on concentrations of particular ROS, these do not report on the redox state of the cell – only on the rate of formation of particular ROS, and since they report *via* covalent reaction, they are not reversible, so unsuitable for monitoring. Furthermore, they do not take into account the mechanisms that the cell naturally puts into place for detoxification of ROS (*e.g.* in the presence of an efficient antioxidant system, a rise in ROS may not dramatically impact the redox state of the cell).

Surface enhanced Raman spectroscopy (SERS) offers a viable alternative to fluorescence for cellular imaging. Raman spectroscopy is a technique that allows vibrational modes of individual bonds to be probed optically and is thus rich in chemical information. While Raman scattering is traditionally a weak effect, making it challenging to measure spectra from dilute samples, Raman spectra/scattering of molecules adsorbed on nanoscale metal surfaces can be enhanced by up to 14 orders of magnitude

making measurements from small numbers of molecules achievable. Gold nanoshells (NS) are a class of engineered nanoparticles comprising a silica core coated in a thin layer of gold. NS are ideal substrates for the measurement of SERS in cells since they exhibit strong, tuneable plasmon resonance (the surface confined effect which gives rise to SERS enhancements) in the near IR region where cells absorb poorly and exhibit low autofluorescence.[14] Furthermore we have demonstrated that NS can be used for intracellular SERS and neither reduce cell viability nor cause cell death.[15] The utility of SERS for making intracellular pH measurements has been demonstrated by several groups. Furthermore, this approach has found notable use in the investigation of endosomal pH dynamics.[15-18]

In this paper, we report the development of a system for measurement of intracellular redox potential which offers significant improvements over the state-of-the-art. Our system uses gold NS to measure SERS spectra and as a result is insensitive to quenching. By modifying these NS with molecules whose SERS spectrum changes depending on oxidation state we can accurately measure proportions of oxidised and reduced species and thus calculate the intracellular redox potential. By using these NS in single fibroblast cells we have measured the localised temporal response to both reductive and oxidative stress over a previously unattainable potential range and correlated oxidative changes measured during apoptosis with changes in caspase activity. Using particles has benefits over soluble reporters since particles may be targeted to, and retained in, cellular compartments of interest.

Results and discussion

Two SERS probe molecules 1,8-diaza-4,5-dithia-1,8-di(2-chloro-[1,4]-naphthoquinone-3-yl)octane (NQ) and 2-Mercapto-benzene-1,4-diol (HQ) were used in this work (see supplementary information for synthetic schemes and characterisation data). Both contain quinone moieties and undergo reversible 2 e^-, 2 H^+ redox reactions in buffered aqueous solutions,[19] which result in a change in their structure and hence SERS fingerprint (Fig 1). In addition to redox-active quinone moieties a robust strategy has been developed that permits irreversible chemisorption of the SERS probes to the gold NS.[20] Figure 1 shows the structure of the SERS probe molecules along with their half-wave potentials (as measured by cyclic voltammetry) and redox reaction schemes.
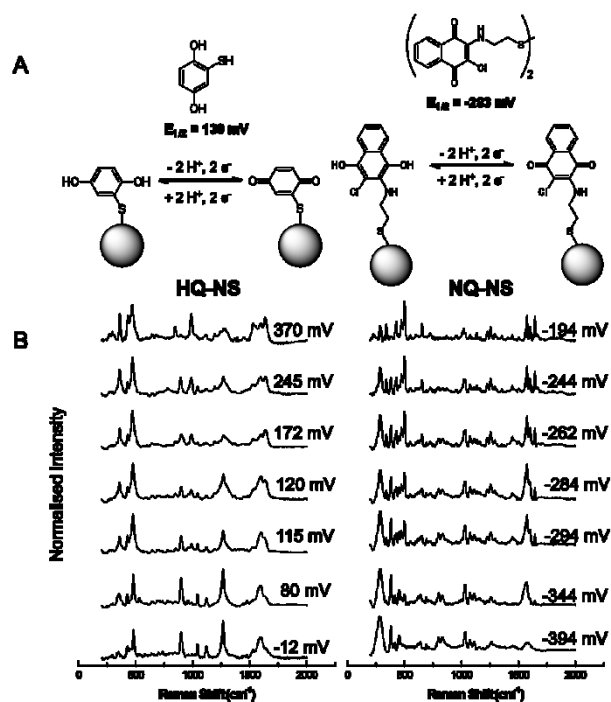
(turn to next page →)

Figure 1. SERS Nanosensors. A – structures, electron transfer schemes and standard reduction potentials; B – potential dependent changes in SERS spectra.

In order to characterise the oxidation-state dependent changes in vibrational modes, we measured SERS spectra across a range of potentials using SERS spectroelectrochemistry. In these experiments, **HQ-NS** or **NQ-NS** were first immobilised on the surface of microfabricated gold electrodes. Using a potentiostat the potential was varied and SERS spectra were recorded from the surface of the gold electrodes to ascertain whether changes in potential could be quantitatively correlated with changes in the SERS fingerprints of the probe molecules.

Figure 1B shows SERS spectra of **HQ-NS** at potentials from -12 mV to 370 mV *vs.* NHE (pH 7.2). The generation of predicted spectra using Density Functional Theory (DFT) at the B3LYP/6-31g(d,p) level, facilitates assignment of observed spectral features to individual vibrational modes of each molecular species (Tables S1 to S2), and these predicted spectra show excellent correlation with the observed spectra. Specifically, several features show a marked, potential dependent, change in intensity and frequency, among these the peak at 357 cm^{-1} corresponds to carbon framework angle bending; the peak at 1263 cm^{-1} corresponds to symmetric ring breathing and the peak at 1585 cm^{-1} which splits from a singlet to a triplet corresponds to the asymmetric ring breathing, C=C stretching and C=O stretching vibrational modes. When the normalised intensity of the peak at 357 cm^{-1} is plotted against potential, the midpoint potential (at which equal amounts of reduced and oxidised species are present) correlates well with the half-wave potential (determined by cyclic voltammetry Figure S3) – this further confirms that the SERS measurement reports accurately on the oxidation

state of the molecule. Similar behaviour can be seen for the other main peaks but since the peak at 357 cm^{-1} is well resolved and high intensity we have used it for further quantification of redox potential.

Similarly, spectra from **NQ-NS** recorded between -394 mV and -194 mV show excellent correlation with DFT calculations (Tables S3 and S4) and, as expected, distinct spectral changes as a function of potential occur at more reducing potentials than those of **HQ-NS**. Vibrational modes which change as a result of oxidation state include the in-plane C-Cl wagging at 280 cm^{-1}, the doublet at 798-833 cm^{-1} which corresponds to aliphatic C-H wagging and aromatic C-H angle bending and the peak at 1577 cm^{-1} which splits from a singlet to a triplet corresponding to symmetric ring breathing, aromatic ring stretching and C=O stretching. The normalised intensity of the peak at 1577 cm^{-1} was chosen for further quantification of redox potential (Figure 2). Again, these spectra show an excellent correlation with the half-wave potential (Figure S4) which confirms that SERS spectra report on the oxidation state of the compound.

A correlation of SERS spectral measurements with predicted values on the basis of cyclic voltammetry is shown in Figure 2.
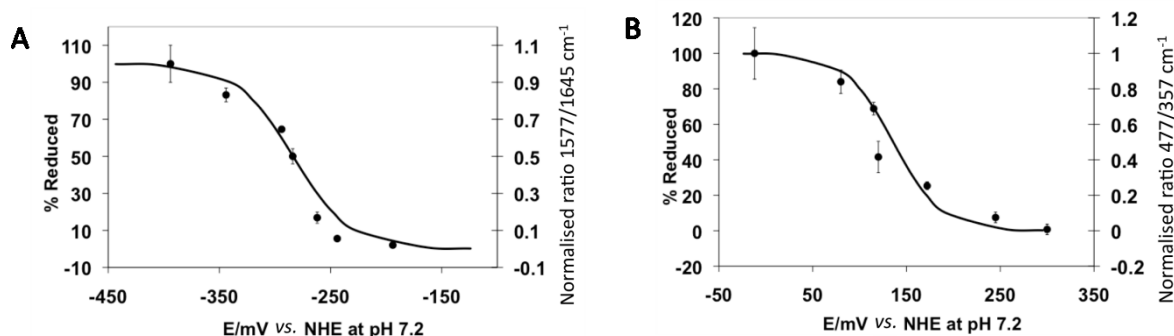
Figure 2. Redox potential ranges covered by SERS nanosensors. A) **NQ-NS** and B) **HQ-NS**. Error bars show the standard deviation of three independent measurements. Points indicate SERS spectroscopic measurements and solid lines represent plots of the Nernst Equation on the basis of half-wave potentials measured using cyclic voltammetry.

In addition to spectroelectrochemical studies we investigated the response of **NQ-NS** to varying ratios of cellular redox couples GSH/GSSG, Cys/CySS and NADP$^+$/NADPH (Figure S5). In each case these cellular redox couples performed electron transfer to or from **NQ-NS**, although in the case of NADP$^+$/NADPH only fully oxidised NADP$^+$ was a strong enough oxidising agent to oxidise **NQ-NS**. This suggests that **NQ-NS** measures a cellular redox state which takes into account more than one redox couple.[21]

Our previous studies using transmission electron microscopy (TEM) have shown that bare NS are taken up by NIH/3T3 fibroblast cells in serum free DMEM growth media and that they are principally located in the cytoplasm, free of lipid coating.[15] While the exact mechanism of uptake remains a subject of investigation, our previous work has also indicated that uptake is independent of energy, cholesterol and clathrin. We have used the same culture conditions to study uptake of **HQ-NS** and **NQ-NS** by NIH/3T3 fibroblast cells. TEM (Figures 3A and S6) confirmed that when modified NS were taken up under these culture conditions, they were predominantly in the cytoplasm and neither encapsulated in vesicles nor coated in lipids. These findings are in agreement with previous studies of nanoparticle uptake which found that nanoparticles can enter cells through a variety of pathways resulting in accumulation in the cytoplasm and may be linked to physical factors such as electrostatics or Van der Wals forces.[22,23,24] While this finding demonstrates that correct control of conditions may allow nanosensors to sense cytoplasmic redox potential, targeting to other organelles is likely to require tuning of the surface chemistry with small molecules[25] or peptides.[26,27]
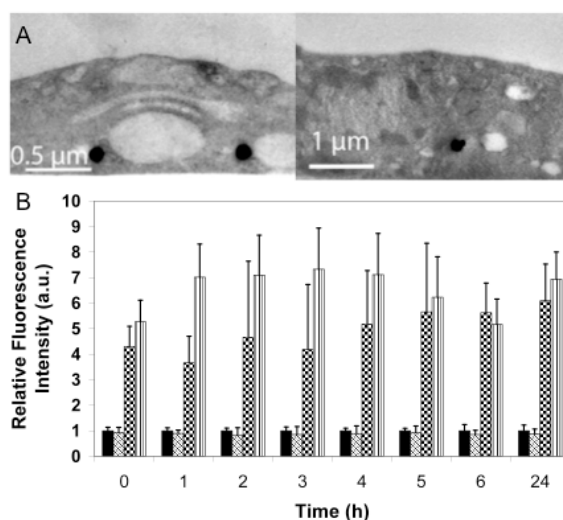
Figure 3. A)TEMs of nanosensors in 3T3 fibroblast cell B) Oxidative stress measured over 24 hours using DCFH-DA assay: Untreated cells (solid bar) Cells incubated with nanosensors (diagonally striped bar) Zn +ve control (chequered bar) t-BOOH +ve control (vertically striped bar).

Since our goal is to use modified nanoparticles to *monitor* changes in redox potential within a cell, it is important to establish that the introduction of such particles to the cell does not *induce* changes in redox potential. In order to investigate this aspect we employed a standard assay of oxidative stress, the DCFH-DA fluorometric assay, in which the generation of ROS leads to a measurable fluorescent signal.[12] We carried out this assay on cells which had been incubated with functionalised NS in serum

free media for 5 hours. Untreated cells (-ve control) and cells which had been treated with either nanoparticulate zinc (1 mg/ml) or tertiary butyl peroxide (t-BuOOH) (0.5 mM) (well established +ve controls) were also included for comparison. Results from the DCFH-DA assay clearly show that while, as expected, Zn and t- BOOH induced a strong oxidative change in the cells, NS did not induce any detectable oxidative changes over a 24 h time period (Figure 3B). The result of this assay confirms that modified NS do not themselves induce formation of reactive oxygen species in mouse fibroblast cells. Furthermore, we carried out assays to measure cellular glutathione status on the basis of concentrations of glutathione and glutathione disulfide. Our results demonstrated that there is no detectable, significant difference in the percentage of reduced *vs.* oxidised glutathione – 3.1% in untreated cells and 2.8% in nanosensor treated cells confirming that the redox status of the cell is unperturbed by treatment with nanosensors.

Using both **NQ-NS** and **HQ-NS**, cytoplasmic redox potentials in live cells were measured. Since the laser focal diameter is 2.1 μm we can collect spectra with subcellular resolution since a typical 3T3 fibroblast cell has a diameter of between 10 and 20 μm. In all cases SERS spectra were collected from the cytoplasm of the cell since our TEM indicate that this is where the nanosensors are located. As expected, **HQ-NS** is fully reduced under conditions of normal cellular physiology and so can be considered insensitive in this potential window. However, **NQ-NS** is approximately 36 % reduced at resting cellular potential. This correlates with a potential of -290 mV *vs.* NHE and is in good agreement with previously reported cytosolic potentials ranging from -315 to - 280 mV *vs.* NHE.[8] Figure 4A shows the measured potential of **NQ-NS** over a 20 min period and confirms that the potential is not only invariant while making measurements over this period but is similar throughout the three independent measurements made.
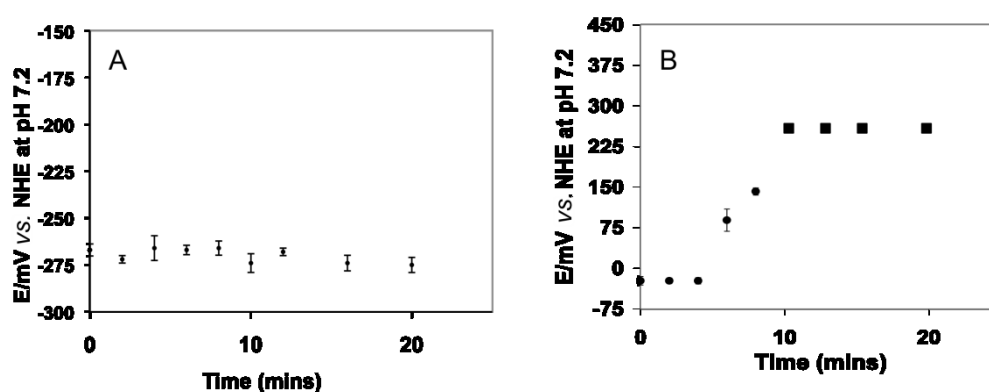

Figure 4. A) **NQ-NS** as a sensor for normoxic cellular potential measurements. B) **HQ-NS** as a sensor of oxidative stress caused by AAPH. Solid squares indicate potentials where HQ-NS is fully oxidised. Error bars indicate the standard deviation of potentials calculated from spectra recorded during three independent experiments.

Since **HQ-NS** is sensitive to potentials outside those found in normal cellular physiology its utility was investigated using conditions known to cause oxidative stress in the cell. Oxidative stress was induced using 2,2'-azobis-2-methyl-propanimidamide, dihydrochloride (AAPH) (30 mM) – a membrane permeable free radical initiator which generates a variety of ROS species through the oxidative stress pathway and which is known to cause oxidative damage to lipids, DNA and proteins.[28] From Figure 4B it can be seen that only 6 mins after addition of AAPH to tissue culture media, there is a measurable change in the cytoplasmic redox potential. The measured potentials are significantly more oxidative than those within the redox buffering range of the glutathione system, indicating that this degree of oxidative stress leads to an irreversible perturbation of the cell potential beyond that of its natural antioxidant system. Generation of superoxide by AAPH and its subsequent conversion to hydrogen peroxide (by SOD) are both known to proceed with rate constants in the order of 10^9 $M^{-1}s^{-1}$. It is therefore likely that the rapid formation of hydrogen peroxide leads to complete oxidation of the cell's quota of glutathione resulting in a fast change in intracellular redox potential as observed here.

In order to maximise the potential range over which we can monitor, we combined the reductive sensitivity of **NQ-NS** with the oxidative sensitivity of **HQ-NS** and carried out a series of measurements under both oxidative and reductive stress. The combination of **NQ-NS** and **HQ-NS** means that the cytoplasmic potential can be monitored across a total of 450 mV – a previously unattainable range in a rapid and reversible manner with a gap of *ca.* 200 mV between the two sensors (Fig. 5). This functional range encompasses the hypoxic conditions in which tumors reside in order to avoid cell death mechanisms at one extreme and the oxidative conditions which are associated with a variety of inflammatory and degenerative disorders and ultimately cell death at the other. For comparison roGFP can monitor from approximately -325 mV to -195 mV.[11]
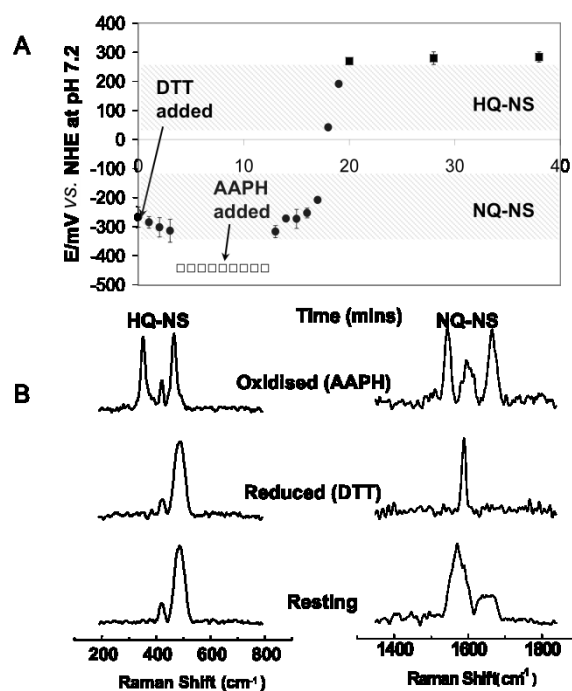
Figure 5. A) Intracellular redox potential measurements using both **NQ-NS** and **HQ-NS** during addition of DTT and AAPH. Shaded areas indicate the areas of the electrochemical window in which **NQ-NS** and **HQ-NS** are sensitive. White squares represent points in which **NQ-NS** is fully reduced and therefore insensitive to further reductive changes and black squares represent points in which **HQ-NS** is fully oxidised and therefore insensitive to further oxidative changes. B) Representative spectra from single cells.

Upon addition of 1 mM Dithiothreitol (DTT), a membrane permeable strong reducing agent,[29] reductive changes in the cell are measurable after only 1 minute. After 4 minutes **NQ-NS** is fully reduced indicating that the potential is at least -350 mV. AAPH (added at 8 mins) induces an oxidative change in the cell which can initially be quantified through monitoring the SERS spectrum of **NQ-NS**. Oxidative changes are measurable at 13 mins and the cytoplasm becomes progressively more oxidative to the extent that **NQ-NS** is fully oxidised (17 mins, redox potential = -208 mV), at which point further oxidative changes can be monitored using **HQ-NS**. The data from **HQ-NS** shows an increasingly oxidative environment and also an increased rate of oxidative change which is to be expected since this potential region is beyond the "redox buffering" capacity of the GSH/GSSG pair. By 20 mins **HQ-NS** is fully oxidised indicating that the potential is at least 250 mV *vs.* NHE and maintains this status throughout the remainder of the experiment. Control experiments using DTT and AAPH in tissue culture media (without cells) show no significant changes to **NQ-NS** or **HQ-NS** spectra confirming that neither reagent reacts in an irreversible manner with either nanosensor.

Furthermore, both **NQ-NS** and **HQ-NS** are fully oxidised under ambient conditions demonstrating that the cell is more reducing than the ambient environment.
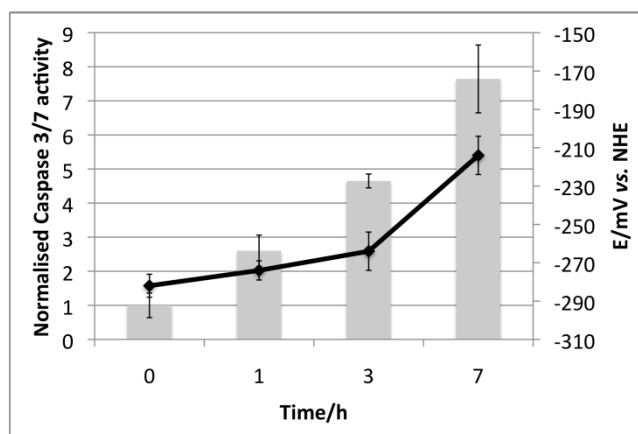

Figure 6. Intracellular potential measurements and caspase activity from mouse fibroblast cells undergoing hydrogen peroxide induced apoptosis. Diamonds represent potential measurements and columns represent measurements of caspase 3/7 activity. Error bars in potential measurements represent the standard deviation across ten single-cell measurements and error bars in caspase activity represent standard deviation across ten replicate wells.

It is notable that spectra collected show good resolution and have no measurable contribution from spectra of other cellular constituents. This is similar to results found when using SERS to measure intracellular pH,[15] and probably reflects the large difference in Raman cross section between the reporter molecules and biomolecules such as proteins and nucleic acids and also the greater proximity of the reporter molecules to the surface compared to other components of the cell. On the basis of TEM experiments, we believe that these spectra are generated by either small aggregates or single NS (Figures 3 and S6) and since our redox potential measurements depend on the ratio of peak intensities and not on absolute intensity they are insensitive to aggregation.

While the above data demonstrate the utility of **HQ-NS** and **NQ-NS** to monitor superphysiological stresses, we have also used **NQ-NS** to measure the oxidative changes which occur in cells as a result of apoptosis (physiological programmed cell death). Apoptosis was induced with hydrogen peroxide at a concentration (500 μM) which we determined to be cytotoxic using an established apoptosis assay and both redox potential and activity of caspases 3 and 7 monitored. Caspases 3 and 7 are key proteolytic effectors of mitochondrial and receptor mediated apoptosis whose activity is regulated by upstream oxidative changes to caspase 9.[30,31] Hydrogen peroxide is the cell's most abundant and

longest lived ROS and is considered to be an important physiological signalling molecule.[2] Figure 6 demonstrates that the intracellular redox potential became progressively more oxidative over the 7 hours immediately following treatment with hydrogen peroxide and that the oxidative changes correlated with an increase in caspase 3 and 7 activity. A control population of cells, untreated with hydrogen peroxide underwent no statistically significant oxidative changes over the same timescale. These measured changes in redox potential are in agreement with measurements of apoptotic potentials made using an assay based on measurement of glutathione oxidation.[8] The data in Figure 6 demonstrate the correlation between redox potential, protease activity and cellular phenotype and underline the critical interplay between redox potential and physiological processes.

Conclusions

The data presented here demonstrate an optical, nanoscale device for monitoring intracellular redox potential which has significant advantages over established techniques. The devices which we have developed report on their local environment and since the vibrational modes of both the oxidised and reduced forms of the small-molecule reporters are represented in the SERS spectrum, the relative proportions of oxidation states can be determined in order to quantitatively calculate the redox potential using the Nernst equation (Figure 2). The ability to quantitatively measure the electrochemical conditions inside the cell is a distinct advantage over the majority of fluorescent alternatives which measure relative amounts of ROS through irreversible covalent reactions which (usually) increase their fluorescence. It is worth noting that, similar to roGFP, electron transfer in both NQ-NS and HQ-NS is coupled to proton transfer which makes the equilibrium position sensitive to changes in pH. Our approach to monitoring redox potential is entirely complementary to a previously reported SERS approach to pH measurements using small-molecule decorated NS and we have previously demonstrated its utility for cellular measurements.[15,16] While the TEMs in Figures 3 and S6 demonstrate that using our current conditions, we can selectively deliver nanosensors to the cytoplasm, we believe that there is considerable scope to tune the particle size and surface chemistry in order to study the effects of redox disregulation in other organelles.[32-35] In the development of new sensing modalities, it is important to establish that the act of making a measurement does not unduly perturb the cell. We have used a variety of assays to establish that these nanosensors which we have developed for intracellular use are non-toxic, previously demonstrating that they do not perturb cell viability or induce cell death.[15] In this paper we have also shown, using two independent assays of oxidative stress that the nanosensors do not induce oxidative changes (Figure 3B), this is further supported by our intracellular spectroscopic measurements which show that intracellular redox potential is invariant throughout a period of regular monitoring (Figure 4A). While certain nanomaterials, such as titanium dioxide fibres and long carbon nanotubes,[36] are known to cause toxicity to cells and animals, gold nanoparticles have been used therapeutically since the 1930s as a

treatment for rheumatism and it is therefore not surprising that gold NS appear to be similarly nontoxic. The two sensors demonstrated here cover a large potential range and they respond to intracellular changes in a fast, reversible and reproducible manner capable of monitoring superphysiological and physiological changes including those associated with caspase activation and apoptosis. While the potential window covered by these sensors is significantly larger than that covered by fluorescent proteins, there is a need for further sensors sensitive in other parts of the cellular electrochemical window. In this regard, an advantage of using small organic molecules rather than proteins is that their standard potential can be tuned relatively easily and predictably using a range of standard synthetic modifications. We are currently investigating this approach. Furthermore, an advantage of using a sensor which is not genetically encoded is that it is less likely to suffer from degradation by proteolysis and is more amenable to use for *in vivo* imaging.

Experimental methods

Spectroelectrochemistry and solution studies: 3-Mercatopropionic acid (2 μl of a 5 mM ethanolic solution) was deposited on the surface of gold microfabricated electrodes which were incubated overnight at rt. The electrodes were carefully rinsed with water and allowed to dry at room temperature. Aqueous EDC solution (2 μl of a 24 mM solution) was then deposited on the surface of the electrodes which were incubated for 30 min at rt. The electrodes were again rinsed carefully with water and allowed to dry at room temperature. Poly-L-lysine solution (2 μl of a 0.1% (w/v) solution) was then deposited on the surface of the electrodes which were incubated for 6 h at rt. After this time, NS (2 μl of a 10 fM solution) were deposited on the electrodes which were subjected to a further wash-dry step. SAMs of the quinone derivatives were formed on the NS by pipetting 2 μl of aqueous solutions of HQ or NQ onto the NS. As with the cyclic voltammetry, solutions of NQ, were incubated with 5mM TCEP. All electrodes were then carefully rinsed with water in order to remove any loosely adsorbed molecules and left to dry at room temperature. Once functionalised with HQ and NQ the gold microfabricated electrodes, along with a coiled platinum wire (0.1 mm diameter) serving as the auxiliary electrode and coiled silver wire (0.5 mm diameter) serving as the reference electrode were connected to a portable potentiostat. The pseudo-reference electrode was calibrated using potassium ferricyanide and found to have a potential of 258 mV *vs.* NHE, all measured potentials were calculated *vs.* NHE for consistency. The electrodes were inserted into a 20 ml glass Petri dish which was charged with phosphate buffer (0.1 M, pH 7.5, 0.1 M KCl). SERS spectra were then recorded at varying potentials. SERS spectra were acquired over 10 s and between a Stokes Raman shift range of 200-1800 cm^{-1}. The same electrodes were used for studies using solutions of redox couples in solution. In this case the electrodes were not connected to a potentiostat and SERS measurements were made while incubating the electrodes in solutions in which the ratio of reduced *vs.* oxidised forms was varied. Solution measurements were carried out in phosphate buffer (100mM, pH 7.2).

Cell Culture: NIH/3T3 mouse fibroblast cells were cultured in Dulbecco's Modified Eagle's Medium (DMEM) supplemented with penicillin/streptomycin (10,000 units/ml), L-glutamine (200 mM) and 10% heat-inactivated calf serum (CS). Cells were incubated at 37 ºC and 5% CO2 in a humidified incubator.

Intracellular SERS Experiments: Cells were seeded at around 50 % confluence on $25 \times 25 \times 1$ mm quartz coverslips (UQG Optics Ltd, UK) and incubated overnight at 37 ºC and 5% CO2 in a humidified incubator in CS free media. Functionalised NS were added to serum-free DMEM (to a final concentration of 10 fM) and were taken up by the cells over a 5 h incubation.[15] Non-adsorbed NS were removed by washing in PBS. Spectroscopic studies were carried out in a temperature-controlled sealed cell in which cells were covered in DMEM. In order to induce oxidative stress in cells, 2,2′ Azobis-2-amidinopropane (AAPH) was introduced into the media at a concentration of 30 mM. In order to induce reductive changes in cells, dithiothreitol (DTT) was introduced into the media at a concentration of 1 mM. In order to induce apoptosis in cells, hydrogen peroxide (500 μM) was introduced into the media for between 1 and 7 h incubations. The cytotoxicity of this dose of hydrogen peroxide was determined using the Apopercentage assay (Biocolor Lifescience). For intracellular studies with **HQ-NS**, SERS spectra were acquired over 30 s between a Stokes Raman shift range of 190-790 cm^{-1}. All spectra were processed using WIRE^{TM} 2.0 software. For intracellular studies with **NQ-NS**, SERS spectra were acquired over 30 s between a Stokes Raman shift range of 1340-1840 cm^{-1}. For both nanosensors fluorescent backgrounds were minimal and corrected using a simple baseline correction. All spectra were processed using WIRE^{TM} 2.0 software.

SERS Microscopy: All SERS spectra were recorded with a Renishaw inVia Raman microscope Raman Spectrometer. A 785 nm diode laser with ~6 mW power at the sample was used along with a $50 \times$ Olympus Long Working Distance objective (NA = 0.45) to focus laser light onto the sample. The focal diameter was 2.1 μm. NS were purchased from Nanospectra Biosciences, Inc. and had a 125 nm silica core and a 25 nm gold shell thickness.

TEM Microscopy: Cells were grown to confluence on Agar Scientific Thermanox cover slips (10.5 × 22 mm) and were incubated overnight with NS (10 fM) in CS free media. The cells were washed three times with PBS and were fixed for 2 h in 3% (v/v) glutaraldehyde in 0.1 M sodium cacodylate buffer. The cells were then washed three times with 0.1 M sodium cacodylate buffer, followed by post fixation overnight with 1% (w/v) osmium tetroxide in 0.1 M sodium cacodylate buffer. The cells were washed with 0.1 M sodium cacodylate buffer, then dehydrated with acetone (50%-100% in steps of 50%, 70%, 90% and 100 %) and then infiltrated and embedded in epoxy resin. Ultra thin sections of the sample were taken using a diamond knife. The sections were positioned on grids and stained with 2 % aqueous uranyl acetate. The grids were then examined and photographed at an accelerating voltage of 80 keV in a CM120 Biotwin (Philips) transmission electron microscope connected to a digital camera.

Assays of oxidative stress: A 96-well plate divided into four sections (untreated cells, 1500 NS/cell, t-BOOH +ve control and Zn +ve control was seeded at a density of 12000 cells per well in DMEM supplemented with penicillin/streptomycin (10,000 units/ml), L-glutamine (200 mM) and 10% CS. The cells were grown to 60% confluence overnight, the media was changed to 2% CS DMEM and the cells left to grow on overnight. The media was removed and the cells washed three times with PBS. Phenol-red free DMEM 0% CS (100 μl) was added to each well along with DCFH-DA (100 μl of a 40 μM solution). The plate was incubated at 37 ºC and 5% CO2 in a humidified incubator for 30 mins. Sample solutions (blank media, NS (10 fM), t-BOOH +ve control (1 mM) and Zn +ve control (1 mM) (200 μl)) were added to the wells containing cells. Fluorescence measurements were taken over a 24 h period at intervals of 0, 1, 2, 3, 4, 5, 6 and 24 h using a BioTek Synergy HT plate reader (excitation 485/20, emission 530/25 nm). Glutathione and protein levels were calculated, in triplicate, from the cytosolic extracts of NIH/3T3 mouse fibroblast cell populations grown in the wells of a 96-well plate at a density of 12000 cells/well. The procedures outlined by Teitze and Smith *et al* were followed in order to determine cellular glutathione and protein levels respectively.[37,38]

Caspase Assays: Caspase 3/7 activity was measured using Apo-ONE Homogeneous Caspase-3/7 Assay from Promega.

NS Functionalisation: NS were functionalised *via* overnight incubation of 1mM solutions of HQ and NQ at rt. Solutions of HQ were aqueous, whereas NQ were water:EtOH mixtures (9:1) and contained 5 mM TCEP. All NS were washed twice with deionised water after functionalisation.

References

[1] Menon, S.G.; Goswami, P.C. A Redox Cycle within the Cell Cycle: Ring in the Old with the New *Oncogene* **2007**, *26*, 1101-1109.

[2] Carroll, K.S.; Paulsen, C.E. Orchestrating Redox Signaling Networks through Regulatory Cysteine Switches *ACS Chemical Biology* **2010**, *5*, 47-62.

[3] Rybicka, J.M.; Balce, D.R.; Khan, M.F.; Krohn, R.M.; Yates, R.M. NADPH Oxidase Activity Controls Phagosomal Proteolysis in Macrophages through Modulation of the Lumenal Redox Environment of Phagosomes *Proc. Natl. Acad. Sci. USA* **2010**, *107*, 10496–10501.

[4] Liu, J.; Cao, L.; Chen, J.; Song, S.; Lee, I.; H. Quijano, C.; Liu, H.; Keyvanfar, K.; Chen, H.; Cao, L.Y. *et al* Bmi1 Regulates Mitochondrial Function and the DNA Damage Response Pathway *Nature* **2009**, *459*, 387-392.

[5] D'Autréaux, B.; Toledano, M.B. ROS as Signalling Molecules: Mechanisms That Generate Specificity in ROS Homeostasis *Nature Rev. Mol. Cell. Biol.* **2007**, *8*, 813-824

[6] Wright, A.F.; Chakarova, C.F.; Abd El-Aziz, M.M.; Bhattacharya, S.S. Photoreceptor Degeneration: Genetic and Mechanistic Dissection of a Complex Trait *Nature Rev. Genet.* **2010**, *11*, 273-284.

[7] Dewhirst, M.W.; Cao, Y.; Moeller, B. Cycling Hypoxia And Free Radicals Regulate Angiogenesis And Radiotherapy Response *Nature Rev. Cancer* **2008**, *8*, 425-437

[8] Kemp, M.; Go, Y-M.; Jones, D.P. Nonequilibrium Thermodynamics of Thiol/Disulfide Redox Systems: A Perspective on Redox Systems Biology *Free Radical Biology & Medicine* **2008**, *44*, 921-937.

[9] Hwang, C.; Sinskey, A.J.; Lodish, H.F. Oxidized Redox State of Glutathione in the Endoplasmic Reticulum *Science* **1992**, *257*, 1496-1502.

[10] Gutscher, M.; Pauleau, A.L.; Marty, L.; Brach, T.; Wabnitz, G.H.; Samstag, Y.; Meyer, A.J.; Dick, T.P. Real-Time Imaging of the Intracellular Glutathione Redox Potential *Nature Meth.* **2008**, *6*553-6559.

[11] Lohman, J.; Remington, S.R. Development of a Family of Redox-Sensitive Green Fluorescent Protein Indicators For Use in Relatively Oxidizing Subcellular Environments *Biochemistry* **2008**, *47*, 8678-8688.

[12] Wang, H.; Joseph, J.A. Quantifying Cellular Oxidative Stress by Dichlorofluorescein Assay Using Microplate Reader *Free Radical Biology & Medicine* **1999**, *27*, 612-616.

[13] Kundu, K.; Knight, S.F.; Willett, N.; Lee, S.; Taylor, W.R.; Murthy, N. Hydrocyanines: A Class of Fluorescent Sensors That Can Image Reactive Oxygen Species in Cell Culture, Tissue, And In Vivo *Angew. Che. Int. Ed.* **2009**, *48*, 299-303.

[14] Jackson, J.B.; Halas, N.J. Surface-enhanced Raman Scattering on Tunable Plasmonic Nanoparticle Substrates *Proc. Nat. Acad. Sci. USA* **2004**, *101*, 17930-17935.

[15] Ochsenkuhn, M.A.; Jess, P.R.; Stoquert, H.; Dholakia, K.; Campbell, C.J. Nanoshells For Surface-enhanced Raman Spectroscopy in Eukaryotic Cells: Cellular Response And Sensor Development *ACS Nano* **2009**, *3*, 3613-3621.

[16] Bishnoi, S.W.; Rozell, C.J.; Levin, C.S.; Gheith, M.K.; Johnson, B.R.; Johnson, D.H.; Halas, N. J. All-Optical Nanoscale pH Meter *Nano letters* **2006**, *6*, 1687-1692.

[17] Nowak-Lovato, K. L. Wilson, B. S.; Rector, K. D. SERS Nanosensors That Report pH of Endocytic Compartments During FcεRI Transit *Analytical and bioanalytical chemistry* **2010**, *398*, 2019-2029.

[18] Kneipp, J. Kneipp, H. Wittig, B.; Kneipp, K. Following the Dynamics of pH in Endosomes of Live Cells With SERS Nanosensors *The Journal of Physical Chemistry C* **2010**, *114*, 7421–7426.

[19] Quan, M.; Sanchez, D.; Wasylkiw, M.F.; Smith, D.K. Voltammetry of Quinones in Unbuffered Aqueous Solution: Reassessing the Roles of Proton Transfer and Hydrogen Bonding in the Aqueous Electrochemistry of Quinones *J. Am. Chem. Soc.* **2007**, *129*, 12847–12856.

[20] Ulmann, A. Formation And Structure of Self-Assembled Monolayers *Chem. Rev.* **1996**, *96*, 1533-1554.

[21] Schafer, F.Q.; Buettner, G.R. Redox Environment of the Cell As Viewed Through the Redox State of the Glutathione Disulfide/Glutathione Couple *Free Radical Biology & Medicine* **2001**, *30*, 1191-1212.

[22] Geiser, M.; Rothen-Rutishauser, B.; Kapp, N.; Schürch, S.; Kreyling, W.; Schulz, H.; Semmler, M.; Hof, V. I.; Heyder, J.; Gehr, P. Ultrafine Particles Cross Cellular Membranes by Nonphagocytic Mechanisms in Lungs and in Cultured Cells *Environmental Health Perspectives* **2005**, *113*, 1555-1560

[23] Rothen-Rutishauser, B.; Mühlfeld, C.; Blank, F.; Musso, C.; Gehr, P. Translocation of Particles And Inflammatory Responses after Exposure to Fine Particles And Nanoparticles in an Epithelial Airway Model *Particle and fibre toxicology* **2007**, *4*, 1-9.

[24] Schaeublin, N. M. Braydich-Stolle, L. K. Schrand, A. M. Miller, J. M. Hutchison, J. Schlager, J. J.; Hussain, S. M. Surface Charge of Gold Nanoparticles Mediates Mechanism of Toxicity *Nanoscale* **2011**, *3*, 410-20.

[25] Sheu, S.S.; Nauduri, D.; Anders, M.W. Targeting Antioxidants to Mitochondria: a New Therapeutic Direction *Biochimica et Biophysica Acta* **2006**, *1762*, 256 –265.

[26] de la Fuente, J.M.; Berry, C.C.; Riehle, M.O.; Curtis, A.S.G. Nanoparticle Targeting at Cells *Langmuir* **2006**, *22*, 3286-3293.

[27] Kang, B.; Mackey, M.A.; El-Sayed, M.A. Nuclear Targeting of Gold Nanoparticles in Cancer Cells Induces DNA Damage, Causing Cytokinesis Arrest And Apoptosis *J. Am. Chem. Soc.* **2010**, *132*, 1517-1519.

[28] Niki, E. Free Radical Initiators As Source of Water Or Lipid Soluble Peroxyl Radicals. *Methods Enzymol.* **1990**, *186*, 100-108.

[29] Cleland, W.W. Dithiothreitol, a New Protective Reagent for SH Groups *Biochemistry* **1964**, *3*, 480– 482.

[30] Lakhani, S.A; Masud, A.; Kuida, K.; Porter, G.A; Booth, C.J.; Mehal, W.Z.; Inayat, I.; Flavell, R.A. Caspases 3 And 7: Key Mediators of Mitochondrial Events of Apoptosis *Science* **2006**, *311*, 847-851.

[31] Zuo, Y.; Xiang, B.; Yang, J.; Sun, X.; Wang, Y.; Cang, H.; Yi, J. Oxidative Modification of Caspase-9 Facilitates Its Activation *via* Disulfide-mediated Interaction with Apaf-1 *Cell research* **2009**, *19*, 449-457.

[32] Murphy, M.P.; Smith, R.A.J. Targeting Antioxidants to Mitochondria by Conjugation to Lipophilic Cations *Annu. Rev. Pharmacol. Toxicol.* **2007**, *47*, 629-656.

[33] Tkachenko, A.G.; Xie, H.; Liu, Y.; Coleman, D.; Ryan, J.; Glomm, W.R.; Shipton, M.K.; Franzen, S.; Feldheim, D.L. Cellular Trajectories of Peptide-Modified Gold Particle Complexes: Comparison of Nuclear Localization Signals and Peptide Transduction Domains *Bioconjugate Chem.* **2004**, *15*, 482-486.

[34] Gordillo, G.; Fang, H.; Park, H.; Roy, S. Nox-4–Dependent Nuclear H_2O_2 Drives DNA Oxidation Resulting in 8-OHdG as Urinary Biomarker And Hemangioendothelioma Formation *Antioxidant Redox Signal.* **2010**, *12*, 933-943.

[35] Zhang, K.; Kaufman, R.J. From Endoplasmic-Reticulum Stress to the Inflammatory Response *Nature* **2008**, *454*, 455–462.(36) Poland, C.; Duffin, R.; Kinloch, I.; Maynard, A.; Wallace,

W.A.H.; Seaton, A.; Stone, V.; Brown, S.; Macnee, W.; Donaldson, K. Carbon Nanotubes Introduced into the Abdominal Cavity of Mice Show Asbestos-Like Pathogenicity in a Pilot Study *Nature Nanotech.* **2008**, *3*, 423-428.

[36] Teitze, F. Enzymic Method for Quantitative Determination of Nanogram Amounts of Total And Oxidized Glutathione: Applications to Mammalian Blood and Other Tissues *Anal. Biochem.* **1969**, *27*, 502-522.

[37] Smith P.K.; Krohn, R.I.; Hermanson, G.T.; Mallia, A.K.; Gartner, F.H.; Provenzano, M.D.; Fujimoto, E.K.; Goeke, N.M.; Olson, B.J.; Klenk, D.C. Measurement of Protein Using Bicinchoninic Acid *Anal. Biochem.* **1985**, *150*, 76-85.